

Threshold Neuron: A Brain-inspired Artificial Neuron for Efficient On-device Inference

Zihao Zheng¹, Yuanchun Li^{1,†}, Jiayu Chen¹, Peng Zhou³, Xiang Chen², Yunxin Liu¹
¹ Tsinghua University ² Peking University ³ LuxiTech

ABSTRACT

Enhancing the computational efficiency of on-device Deep Neural Networks (DNNs) remains a significant challenge in mobile and edge computing. As we aim to execute increasingly complex tasks with constrained computational resources, much of the research has focused on compressing neural network structures and optimizing systems. Although many studies have focused on compressing neural network structures and parameters or optimizing underlying systems, there has been limited attention on optimizing the fundamental building blocks of neural networks – the neurons. In this study, we deliberate on a simple but important research question: Can we design artificial neurons that offer greater efficiency than the traditional neuron paradigm? Inspired by the threshold mechanisms and the excitation-inhibition balance observed in biological neurons, we propose a novel artificial neuron model, Threshold Neurons. Using Threshold Neurons, we can construct neural networks similar to those with traditional artificial neurons, while significantly reducing hardware implementation complexity. Our extensive experiments validate the effectiveness of neural networks utilizing Threshold Neurons, achieving substantial power savings of $7.51\times$ to $8.19\times$ and area savings of $3.89\times$ to $4.33\times$ at the kernel level, with minimal loss in precision. Furthermore, FPGA-based implementations of these networks demonstrate $2.52\times$ power savings and $1.75\times$ speed enhancements at the system level. The source code will be made available upon publication.

1 INTRODUCTION

Artificial intelligence (AI) has showcased exceptional performance and significant influence across diverse domains. Deep Neural Networks (DNNs) have emerged as the dominant technology within AI circles, finding widespread application in a multitude of real-world scenarios [14, 22]. Furthermore, the rise of diffusion models like DALL-E3 [3] and Imagen [33] has unveiled remarkable content generation capabilities, sparking considerable interest and research efforts.

However, efficiency is a widely-concerned problem in the deployment of DNNs. DNNs necessitate significant computational power and memory resources, posing hardware deployment challenges. Pruning-based approaches [30, 48] reduce the number of neurons to limit the resource requirement. Quantization-based methods [17] use a low-precision format

to represent parameters to reduce storage and computing costs. Furthermore, Neural Architecture Search (NAS) is evolving to explore efficient architectures for various tasks without relying on an excessive number of parameters [43]. Certain mobile/edge scenarios, such as IoT tasks and near-sensor processing, require fast and energy-efficient AI computing. Improving the efficiency of DNNs facilitates the deployment of these models on mobile and edge devices, such as mobile phones, FPGAs, and Raspberry Pi, thereby reducing hardware demands [15, 19, 46].

Despite the aforementioned approaches, few efforts are focused on the artificial neurons - the most fundamental data processing units of DNNs. Each unit in DNNs that performs signal processing can be considered as a neuron [35, 40]. From this perspective, existing artificial neurons in modern DNNs include weighted-sum, normalization, rectifier, pooling, and so on. Among them, weighted-sum is the most dominating and inefficient one that is used in linear layers, convolution layers, and attention layers [7, 42].

Traditionally, standard artificial neurons have been designed with a top-down approach that prioritizes model accuracy, often neglecting considerations for hardware efficiency. As accuracy improvements plateau in many domains, this presents an opportunity to explore bottom-up design approaches to develop fundamentally more hardware-efficient artificial neuron paradigms.

Two key limitations in existing artificial neuron designs present opportunities for optimization. **Limitation 1: Heavily dependent on multiplication operations.** The area and power consumption of the circuit required to perform a multiplication operation are the highest among all common operations. Reducing the number of multiplication operations can effectively improve efficiency, and completely removing multiplications from neural networks would be even better, which can significantly reduce chip complexity. **Limitation 2: The use of multiple types of artificial neurons in DNNs results in hybrid circuits in accelerator design.** Traditional DNNs employ various types of artificial neurons, each necessitating a unique circuit design as well as distinct simulation and synthesis processes. This diversity significantly escalates the complexity and time involved in designing neural network accelerators. In contrast, adopting a unified neuron model, such as the Threshold Neuron, can streamline the design process.

Standardizing on a single type of neuron eliminates the need for multiple circuit designs and additional components like normalization layers. This unified approach reduces overall complexity, thereby enhancing the efficiency of the design, simulation, and implementation processes.

Therefore, an ideal design of hardware-efficient artificial neurons should have two features. First, the ideal neurons should rely on hardware-efficient operations instead of heavy multiplications. Second, the ideal neurons should be unified for compact hardware implementation. Although there are a few pioneering studies on reducing multiplications in neural networks, such as AdderNet [7], ShiftAddNet[42], BNN [16], XNOR-Net [27], and Matmul-free[49], they still rely on multiplications (*e.g.* normalization) or need multiple types of neurons to be effective.

To achieve this goal, we draw inspiration from the human brain and attempt to design a unified multiplication-free neuron, since the brain is probably the most powerful and efficient processor. Specifically, we notice two important characteristics of the brain that might be useful for efficiency. **Characteristic 1: Biological neurons have a threshold mechanism.** When the signal from the previous neuron is transmitted, if it is below the threshold, the membrane potential of that neuron will not change [10]. This mechanism not only effectively reduces computational power consumption, but also improves the exclusion of invalid information. **Characteristic 2: Human brains have an excitation-inhibition balance.** The synapses of each neuron in human brains can release different neurotransmitters, which determine whether the next neuron is excited or inhibited. Existing works have already proved that excitation-inhibition balance is the basis of learning and execution capabilities [5, 21, 41]. Existing artificial neurons do not possess these two characteristics.

Based on these insights, we propose a new neuron design named Threshold Neurons. First, we abstract the threshold mechanism inside each neuron, taking the thresholds as the learnable weights. Second, Threshold Neurons use subtractions rather than multiplications to achieve interaction between weights and inputs. Third, we abstract the excitation-inhibition balance into the polarity of Threshold Neurons, enabling the modeling of neurons to reflect this balance and improving the fitting capability of Threshold Neurons.

Additionally, Threshold Neurons are utilized to construct networks within existing architectures, resulting in the creation of the Threshold-Net series. To enhance the training convergence of Threshold-Net, we use a random signal initialization mechanism. Because of multiplication-free designs and the threshold mechanism, the aggregation effect of each layer’s output in Threshold-Net is not salient. As a result, normalization is unnecessary. Due to the inherent non-linearity in neurons, Threshold-Net does not need rectifiers (activation

functions). We also use convolution sampling to replace pooling. These designs make Threshold-Net extremely simple for hardware support while remaining effective in modeling.

According to our experiments on various popular vision and sensing tasks, Threshold-Net can achieve State-of-The-Art (SOTA) accuracy on most tasks with much less heavy computation. Our hardware simulation and FPGA prototype demonstrate the end-to-end power efficiency of our design. We anticipate that dedicated lower-level hardware support will further harness the simplicity and efficiency of Threshold Neurons.

Overall, our contributions are three-fold:

- We propose a new type of neuron called Threshold Neurons. Threshold Neurons are multiplication-free, unified, and brain-inspired, with a proper abstraction of the threshold mechanism and the excitation-inhibition balance.
- We use Threshold Neurons to construct networks, thus forming Threshold-Net. Threshold-Net does not need normalization, rectifier, and pooling, maintaining unity. It can also use existing optimization algorithms for training and updating.
- We evaluate Threshold Neurons and Threshold-Net on various tasks. The results show that Threshold Neurons and Threshold-Net achieve SOTA performance while remaining unified and multiplication-free. Our hardware simulation shows that Threshold Neurons can achieve $7.51\times \sim 8.19\times$ power savings and $3.89\times \sim 4.33\times$ area savings at the kernel level. The FPGA-based implementation shows $2.52\times$ power saving and $1.75\times$ speedup at the system level.

2 BACKGROUND AND MOTIVATION

2.1 DNN Deployment on Mobile/edge Device

Deep neural networks (DNNs) have achieved remarkable results in multiple fields such as image classification [14, 22, 36], object detection [23, 28], sentiment analysis [44], and recommendation systems [9, 47].

A DNN typically consists of multiple stacked blocks, with each block containing similar layers. For instance, as shown in Figure 1(a), a typical block of DNNs consists of three parts: the weighted-sum layer (including the convolution and fully-connected layers), the normalization layer, and the rectifier layer (activation function) [14, 36]. Sometimes, the pooling layers are plugged into the block [22].

Weighted-sum layers are responsible for extracting features from the input data. Normalization layers, such as Batch Normalization (BN), are applied to normalize data, ensuring stable and efficient convergence of the network. Rectifiers (activation functions) introduce non-linearity, which is crucial for enabling deep neural networks to learn complex patterns.

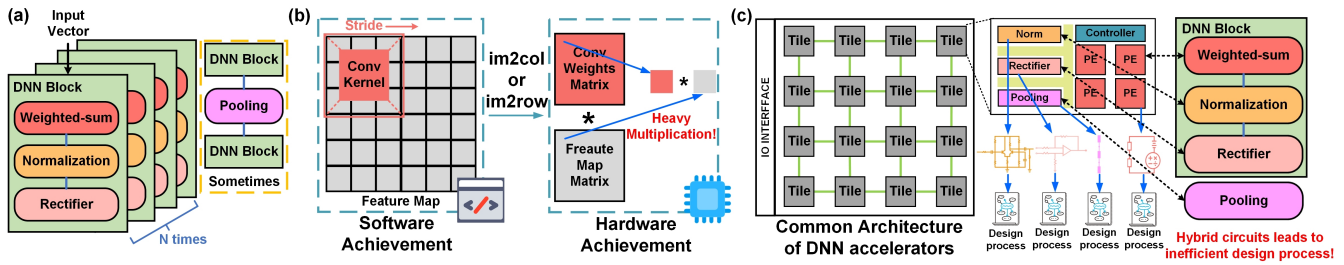


Figure 1: (a) The common architecture (including weighted-sum layer, normalization layer, pooling layer, and rectifier) of DNNs. (b) Comparison between software and hardware implementations of convolution operations. (c) Hybrid circuits in DNN accelerator design.

Pooling layers reduce the dimensionality of feature maps by performing down-sampling, with methods like maximum pooling selecting the highest value within a specified kernel size.

Mobile/edge devices typically have limited storage space and computing power, requiring tasks deployed on them to be low-power and efficient. DNNs are resource-intensive, so deploying DNNs on edge devices faces many problems, such as high memory overhead, slow inference speed, and high power consumption. Improving the efficiency of DNNs is a continuous challenge, as there is a constant demand to handle more tasks with higher quality under increasingly stringent resource constraints.

Meanwhile, the common scenarios of edge DNNs provide a different angle to rethink the optimal trade-offs in network and hardware design. For instance, many edge AI applications deployed on energy-harvesting embedded devices deal with low-dimension sensing data or low-resolution images, which does not require the high fitting ability of the most advanced AI models and operators, while the complex hardware and system for supporting the advanced models/operators may become a heavy burden in such resource-constrained devices. Therefore, an exciting research opportunity in edge AI is the integrated design of models and hardware, achieving higher whole-stack efficiency.

2.2 Problems of Conventional Neurons

The conventional neurons used in modern DNNs face two problems: one is the dependence on multiplications, and the other is the hybrid circuit caused by various neurons.

2.2.1 Dependence on Multiplications. The weighted-sum layers are the most common in DNNs, containing convolution layers and fully-connected layers. For fully-connected layers, the outputs are obtained by multiplying the weight matrix with the input matrix.

In hardware implementations, there are no specialized circuits for directly handling convolution operations with stride

Table 1: The power and area of common operations in hardware circuits. The frequency is limited to 50 MHz. All results come from Synopsys DC, using 28nm TSMC PDK.

Operations	Power (mW)	Area (μm^2)
Multiplication	2.48e-1	488.14
Addition	1.77e-2	58.80
Subtraction	1.77e-2	58.80
Shift	4.8e-3	28.31
OR	7.12e-3	36.06
AND	5.93e-3	36.06
NOT	5.76e-3	32.93
XOR	8.72e-3	40.77
XNOR	8.70e-3	40.77

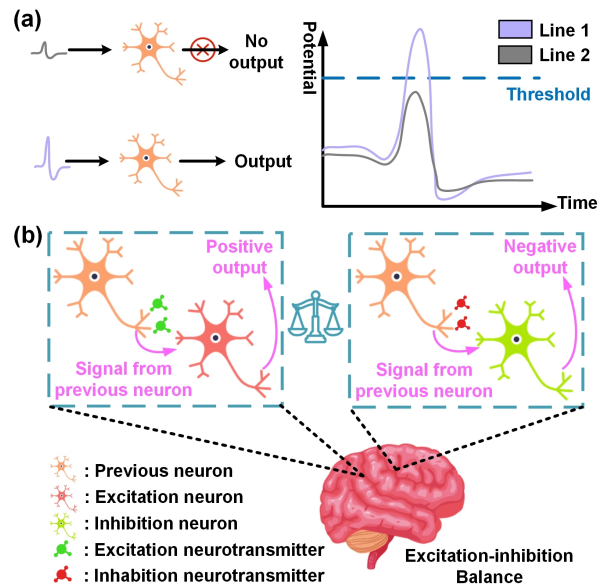


Figure 2: (a) The threshold mechanism in the neurons of human brains. (b) The excitation-inhibition balance in human brains.

windows. As a result, convolution operations are typically converted into equivalent matrix multiplications using the `im2col` or the `im2row` algorithm [12, 32], as shown in Figure 1 (b). This conversion makes multiplication the predominant operation in DNNs.

We select typical computer operations, implement their corresponding circuits, and report their area and power consumption, as shown in Table 1. Table 1 shows that the area and power consumption of multiplication circuits are significantly larger than those of other operations. Therefore, reducing multiplications can save hardware resources and achieve efficient and green AI computing.

2.2.2 Hybrid circuits in accelerator design. Here, we gaze at DNNs from a bottom-up view. Each signal processing unit in DNNs can be seen as a type of neuron. From this perspective, common DNNs comprise multiple types of neurons, including weighted-sum, normalization, pooling, and rectifier. This variety leads to various hardware circuit prototypes. Each circuit prototype needs a corresponding design process, including simulation, synthesis, routing, placing, etc.

A practical instance is in SOTA DNN accelerators [8, 34], Processing Elements (PEs) act as weighted-sum neurons, incurring the main computing cost. Reusing PEs enables a large number of weighted-sum neurons using only one circuit prototype and design process. Nonetheless, even when the computational cost of other neuron types is low, it remains necessary to design separate modules and undertake distinct design processes for each. hybrid circuits make the accelerator design inefficient and complex due to various types of neurons, as shown in Figure 1 (c). If the neurons inside DNNs can be unified (without other types of neurons), it will bring convenience to accelerator design.

2.3 Human Brain Inspirations

Human brains are powerful and efficient. Although the mechanisms leading to such efficiency are unclear yet, we notice two inspirational characteristics. One is the threshold mechanism, and the other is the excitation-inhibition balance.

Threshold Mechanism. Neurons in human brains have a threshold mechanism [10]. When a neuron receives a signal input from presynaptic neurons, it compares the signal with the threshold. If the signal amplitude exceeds this threshold (like Line 1 in Figure 2 (a)), the neuron generates an output. Conversely, if the signal amplitude is below the threshold (like Line 2 in Figure 2 (a)), no output is produced. This threshold mechanism enables the neuron to effectively filter out irrelevant or low-intensity signals, thereby enhancing the efficiency of individual neurons and the overall neural network.

Excitation-inhibition Balance. There are two kinds of neurons in human brains: excitation neurons and inhibition

neurons. Excitation neurons output positive signals and promote the electrical activity of other neurons through their activity. When excitation neurons transmit signals to other neurons, the output positive signal makes it easier for the receiving neuron to generate action potentials. This effect is usually achieved through the release of excitation neurotransmitters [5].

Inhibition neurons output negative signals and their function is to reduce the electrical activity of other neurons. When inhibition neurons send signals to other neurons, the output negative signal makes it more difficult for the receiving neuron to generate action potentials. This effect is usually achieved through the release of inhibition neurotransmitters [41].

Human brains must have both excitation neurons and inhibition neurons simultaneously and maintain their balance, as shown in Figure 2 (b). This balance ensures that neural activity is neither overly excited, leading to abnormal states like epilepsy, nor excessively inhibited, resulting in functional impairment or loss of consciousness. The balance between excitation and inhibition also contributes to efficient neural encoding and information processing, indicating its important role in efficient and economical brain functioning [21].

2.4 Design Goal and Challenges

The aforementioned analysis motivates us to think about an interesting and important research question: **How can we re-design the low-level artificial neurons in DNNs to improve efficiency?**

Addressing this question presents several key challenges. **Challenge 1:** How to reduce the heavy dependence on multiplication operations? Conventional artificial neurons use multiplications to achieve interaction between input signals and weights. Reducing the number of multiplications in neurons will disrupt this process, making it impossible for neurons to perform weighted interactions on input signals. **Challenge 2:** How to unify the types of neurons in a neural network? Normalization, pooling, and rectifiers are indispensable in DNNs. Removing them could result in the invalidation of neurons, potentially causing the entire network to collapse. **Challenge 3:** How to retain the effective learning abilities of such a new form of neural networks? The training scheme and optimization algorithm of DNNs are based on solid theoretical foundations, which are also responsible for the effective learning capability of DNNs. To ensure that newly designed neurons and networks possess strong learning abilities, they must adhere to these theories, which restrict the space of neuron design.

Fortunately, inspired by human brains, we successfully solve all these challenges and eventually design Threshold Neurons. Our design will be detailed in Section 3.

3 DESIGN

3.1 Overview

We propose a new type of artificial neuron called Threshold Neurons to address the problems of existing artificial neurons used in conventional DNNs.

First, as implied by the name, we introduce a threshold mechanism in Threshold Neurons. Each signal from previous neurons will be compared with a threshold. When the amplitude of the signal is higher than the threshold, this neuron will perform calculations and output results. Otherwise, the neuron will have no output. The threshold mechanism effectively filters out insignificant signals, thus enhancing the efficiency of the neurons. Since the major functionality of multiplication operations in conventional neurons also balances the significance of signals from preceding neurons, our design actually replaces the multiplications with threshold-based comparison and subtraction operations, which are significantly more hardware-efficient.

We further develop the Threshold Neuron to get rid of other non-uniform neural operations. After the threshold operations, all signals are aggregated with summation. The aggregated output is relatively smooth, and the corresponding gradients are also relatively stable (without the gradient explosion and vanishing effects produced by weighted-sum operations). With these benefits, networks built using Threshold Neurons do not require normalization. In addition, the threshold mechanism introduces inherent non-linearity in neurons. Therefore, Threshold Neurons do not need separated activation units. We use thresholds as weights of neurons to make them learnable, rather than using constant thresholds, thus enhancing the fitting ability and versatility of Threshold Neurons.

Similar to the conventional artificial neurons, we can use Threshold Neurons to construct networks and design corresponding forward computation and back-propagation mechanisms to enable effective learning. The neural networks constructed with Threshold Neurons are called Threshold-Net. The inherent properties of Threshold Neurons reduce the need to use rectifiers and normalization in Threshold-Net, and we further use convolution to replace pooling operations in Threshold-Net, leading to a fully unified design. To make Threshold-Net trainable and enhance its fitting ability, we divide Threshold Neurons into two polarities and introduce a polarity balance, inspired by the excitation-inhibition balance in human brains. We propose a random polarity initialization scheme in Threshold-Net. Experiment results show that this scheme is effective and Threshold-Net can be trained on different tasks, achieving SOTA performance compared to other baselines.

In the remaining part of this section, we will provide a detailed introduction to the design of Threshold Neurons and Threshold-Net.

3.2 Threshold Neurons

3.2.1 Inspired by The Threshold Mechanism. The model of conventional artificial neurons is shown in Figure 3 (a). This model receives signals X_1, X_2, \dots, X_N from previous neurons. The signals multiply with corresponding weights and then are aggregated by the neuron. After adding a bias term and rectification by the rectifier, the neuron finally outputs the result. This process of artificial neurons can be represented as Formula (1).

$$Y = \phi\left(\sum_{i=0}^N (W_i * X_i) + b\right) \quad (1)$$

Where ϕ represents the rectifier (activation function), W_i represents the weight, and X_i represents the input signal of neurons. N means the number of input signals. Y means the final output of the neuron, and b is the bias term.

Unlike artificial neurons, Threshold Neurons introduce a threshold mechanism and use simple operations to achieve efficient processing. The model of Threshold Neurons is shown in Figure 3 (b). Each input signal X_i is compared with the corresponding threshold. We set the thresholds as the weights, making them learnable during the training process. We use subtractions to achieve the interaction between inputs and weights. The process can be written as Formula (2).

$$T(X_i, W_i) = \begin{cases} X_i - W_i & X_i > W_i \\ 0 & \text{otherwise} \end{cases} \quad (2)$$

Function T represents the process of comparing with the thresholds. When the amplitude of input X_i is higher than that of W_i , the neuron will output the difference of subtraction. After T , signals will be aggregated, then add the bias term b to get the final output Y , as shown in Formula (3).

$$Y = \sum_{i=0}^N (T(X_i, W_i)) + b \quad (3)$$

The model and the Formula (3) show that Threshold Neurons are efficient because of using simple operations rather than multiplications. They have inherent non-linearity, eliminating the need for rectifiers. Moreover, the threshold comparisons and subtractions reduce the aggregation effect, eliminating the need for normalization.

3.2.2 Inspired by Excitation-inhibition Balance. As aforementioned, we succeed in constructing the model of Threshold Neurons. How can we guarantee that each neuron has the appropriate fitting capability? Inspired by excitation-inhibition balance in human brains, we introduce a polarity mechanism and divide Threshold Neurons into positive and negative, as shown in Figure 4. We abstract excitation neurons in human brains as positive Threshold Neurons and inhibition neurons

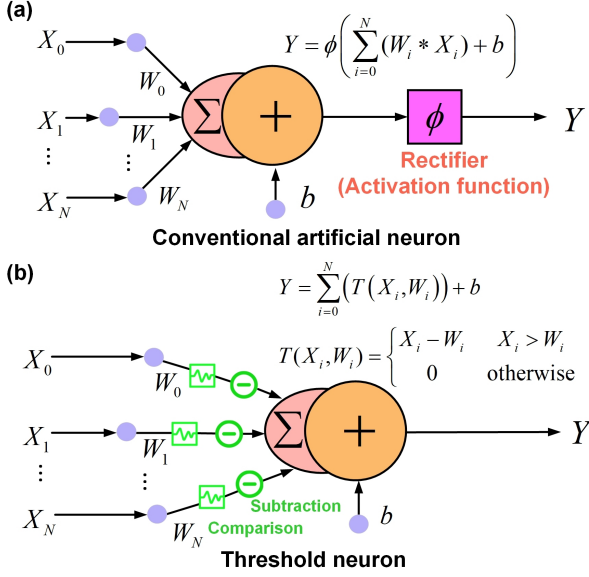


Figure 3: (a) The Model of Conventional Artificial Neurons. (b) The Model of Threshold Neurons.

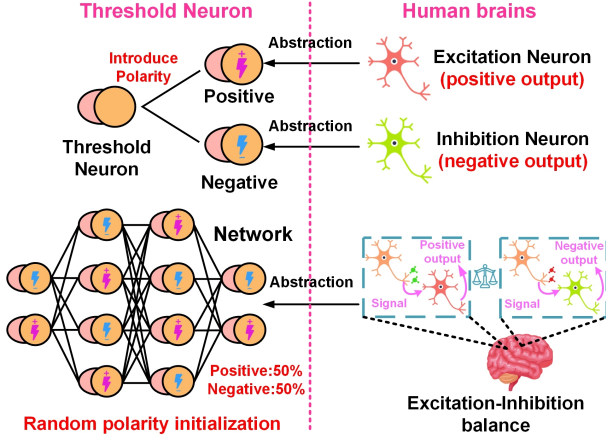


Figure 4: Abstraction of Excitation-inhibition Balance in Threshold Neurons.

in human brains as negative Threshold Neurons. Excitation neurons output positive signals, and inhibition neurons output negative signals. Therefore, we redefine the function T of positive and negative Threshold Neurons, as shown in Formula (4) and Formula (5).

$$\text{Positive} : T_{pos}(X_i, W_i) = \begin{cases} (X_i - W_i) & X_i > W_i \\ 0 & \text{otherwise} \end{cases} \quad (4)$$

$$\text{Negative} : T_{neg}(X_i, W_i) = \begin{cases} -(X_i - W_i) & X_i > W_i \\ 0 & \text{otherwise} \end{cases} \quad (5)$$

In our initial design attempts, polarity initialization was crucial. Unbalanced initialization or uneven initialization can lead to adverse effects, some of which can reduce the fitting ability of Threshold Neurons, while others can make Threshold Neurons lose trainability. Considering these, we use a random polarity initialization scheme. We randomly initialize the polarity of each neuron and keep its polarity unchanged during the training process. When the number of neurons is large enough, the ratio of positive and negative neurons will be around 50%. This scheme ensures that the polarity partition is not only balanced but also even.

3.3 Threshold-Net

Starting from the long-standing tradition of energy-saving hardware implementation, the design of Threshold Neurons is more hardware-efficient than multiplication-based artificial neurons. In this section, we use Threshold Neurons to construct networks and consider how to make the network trainable using the theory and algorithms of DNNs.

3.3.1 Forward Propagation. Consider $F \in \mathbb{R}^{S \times S \times C_{in} \times C_{out}}$ is a filter, which is used as a layer of DNN, where kernel size is S , input channel is C_{in} and out channel is C_{out} . The input figure is represented by $X \in \mathbb{R}^{H \times W \times C_{in}}$. H and W represent the height and width of the input figure map, respectively. The output feature map of $F \in \mathbb{R}^{S \times S \times C_{in} \times C_{out}}$ is represented by Y . The forward propagation of a conventional DNN layer can be written as Formula (6).

$$Y(m, n, t) = \sum_{i=0}^S \sum_{j=0}^S \sum_{k=0}^{C_{in}} T(X(m+i, n+j, k), F(i, j, k, t)) \quad (6)$$

$T(\cdot, \cdot)$ is a pre-defined similarity measure. If cross-correlation is taken as the metric of distance, e.g. $T(x, y) = x \times y$ and $S \neq 1$, the Formula (6) transfers to the convolution operations. When $S = 1$ and $T(x, y) = x \times y$, Formula (6) represents the fully-connected layer. $T(x, y)$ of positive Threshold Neurons and negative Threshold Neurons can be represented as Formula (4) and Formula (5).

In the design of Threshold Neurons, we introduce the polarity and divide the Threshold Neurons into positive and negative. Therefore, when using Threshold Neurons to construct Threshold-Net, there are two types of neurons, leading to different T . We use T_r to unifiedly represent T_{pos} and T_{neg} . So the Formula (6) can be written as Formula (7). When constructing Threshold-Net, the number of neurons is large enough, so the probability distribution of T_r can be expressed as $P(T_r = T_{pos}) = 0.5$ and $P(T_r = T_{neg}) = 0.5$.

$$Y(m, n, t) = \sum_{i=0}^S \sum_{j=0}^S \sum_{k=0}^{C_{in}} T_r(X(m+i, n+j, k), F(i, j, k, t)) \quad (7)$$

From these, we deduce each layer’s computing process of Threshold-Net. Formula (7) shows that Threshold Neurons are compatible with existing forward propagation theory in layer-grained.

3.3.2 Backward Propagation. DNNs use backward propagation to compute the gradient of each layer, and then use optimization algorithms (*e.g.* Stochastic Gradient Descent) to update the weights. In DNNs, the backward propagation of weighted-sum layers can be represented as:

$$\begin{aligned} \frac{\partial Y(m, n, t)}{\partial F(i, j, k, t)} &= \frac{\partial(X(m+i, n+j, k) \times F(i, j, k, t))}{\partial F(i, j, k, t)} \\ &= X(m+i, n+j, k) \end{aligned} \quad (8)$$

where $i \in [m, m+S]$ and $j \in [n, n+S]$. In Threshold-Net, T_{pos} and T_{neg} are differentiable except when $X(m+i, n+j, k) = F(i, j, k, t)$. We define the derivative of this situation as 0 so that T_{pos} and T_{neg} are completely differentiable. Therefore, the backward propagation process can be represented as follows.

$$\begin{aligned} \frac{\partial Y(m, n, t)}{\partial F(i, j, k, t)} &= \frac{\partial T_{pos}(X(m+i, n+j, k), F(i, j, k, t))}{\partial F(i, j, k, t)} \\ &= \begin{cases} \frac{\partial X(m+i, n+j, k)}{\partial F(i, j, k, t)} - 1 & X(m+i, n+j, k) > F(i, j, k, t) \\ 0 & \text{otherwise} \end{cases} \end{aligned} \quad (9)$$

$$\begin{aligned} \frac{\partial Y(m, n, t)}{\partial F(i, j, k, t)} &= \frac{\partial T_{neg}(X(m+i, n+j, k), F(i, j, k, t))}{\partial F(i, j, k, t)} \\ &= \begin{cases} 1 - \frac{\partial X(m+i, n+j, k)}{\partial F(i, j, k, t)} & F(i, j, k, t) > X(m+i, n+j, k) \\ 0 & \text{otherwise} \end{cases} \end{aligned} \quad (10)$$

Therefore, Threshold-Net can seamlessly integrate with the backward propagation theory of DNNs. Threshold-Net can be incrementally updated and optimized using standard DNN training methods. However, some other multiplication-less networks [16, 27] face non-differentiable problems and need to use the Straight Through Estimator (STE) to estimate gradients.

3.3.3 Network Architecture. Threshold Neurons are different from conventional artificial neurons, which makes us reconsider the architecture of Threshold-Net. Overall, there are three changes in Threshold-Net architecture.

Change 1: Normalization-free. The aggregation process in artificial neurons leads to discrete feature maps and increased numerical variances, posing challenges for the network to effectively fit this discrete data distribution. Hence, normalization of the feature maps becomes essential to facilitate the network in capturing the data distribution accurately. In contrast, Threshold Neurons employ subtractions and thresholds before aggregation, which inherently reduce

the numerical disparities. As a result, normalization is unnecessary in Threshold-Net. Given that normalization does not alter the tensor dimension, we opt to eliminate normalization directly from the architecture of Threshold-Net.

Change 2: Rectifier-free. In DNNs, rectifiers must be added between layers to introduce non-linearity. However, Threshold Neurons have natural non-linearity, so rectifiers are not required in Threshold-Net. Rectifiers are usually element-wise and do not change tensor dimension, so we remove rectifiers between layers in Threshold-Net.

Change 3: Pooling-free. DNNs sometimes use pooling for downsampling. There are already works trying to replace pooling in DNN architecture [35]. Inspired by this, we replace pooling layers with convolution layers in Threshold-Net. To maintain the output size of feature maps, we set the convolution kernel size to equal the pooling kernel size. For other parts, we use the existing architecture of DNNs in Threshold-Net.

3.3.4 Integration with Conventional Neural Layers. Although neural networks built exclusively with Threshold Neurons can already attain a good fitting capacity with optimal efficiency, there are situations where sacrificing some efficiency for improved accuracy may be preferable. In this section, we introduce a method to achieve such adaptable trade-offs by integrating Threshold-Net layers with traditional neural layers.

Given the theoretical compatibility between Threshold-Net and traditional DNNs, it is feasible to blend them by mixing Threshold-Net layers with conventional neural layers and training them using the same optimization algorithms. To facilitate this integration, we introduce a layer-based Multiplication Injection (MI) mechanism. This approach allows us to interchange a Threshold-Net layer with a conventional neural network layer, provided that the parameters (*e.g.*, channels, kernel size, etc.) within the layer remain consistent.

This trade-off results in a balance: the greater the MI, the reduced proportion of Threshold Neurons, leading to decreased overall network efficiency but enhanced fitting capability. In practical scenarios, Threshold-Net can be segmented at the layer level. DNN layers can be executed on conventional computing devices (*e.g.* CPU, GPU), while Threshold-Net layers can be processed on specialized hardware. From this standpoint, the utilization of MI does not compromise the unity of Threshold-Net.

Based on MI, we extend Threshold-Net to diffusion models. The diffusion noise comes from a Gaussian noise generator. The U-Net model accepts the noise and gradually learns the noise’s distribution at each time step. We keep the generator normal to ensure that the noise follows a Gaussian distribution. We construct the U-Net model by Threshold-Net and use MI to improve fitting capability. In addition, the thresholds of

Threshold Neurons are learnable, so they will automatically change to fit the Gaussian distribution of the noise. If the thresholds are static, equivalent to fixed bandwidth filters, they will disrupt the Gaussian distribution of diffusion noise.

4 IMPLEMENTATION

This section will introduce how we implement Threshold Neurons and Threshold-Net.

GPU Support for Training. Most existing DNN models are developed and trained using the PyTorch framework on GPUs. Building on this standard, we implement Threshold Neurons as GPU kernels using CUDA to leverage the computational capabilities of modern graphics hardware. To address the complexity associated with modifying individual computing kernels in PyTorch, we implement custom layer functions analogous to the PyTorch API, namely `tConv2d` and `tLinear`. These functions facilitate the construction of our network architecture, enabling users to assemble the Threshold-Net architecture in a manner consistent with traditional DNNs. Once configured, the Threshold-Net is compiled into machine code and executed on GPUs via an interpreter for training purposes. The entire process is illustrated in Figure 5.

During the deployment phase, GPU-based implementations become suboptimal. While GPUs excel in computationally intensive tasks and matrix multiplication, Threshold Neurons do not benefit from these capabilities due to their non-reliance on multiplication operations. The ideal solution is to develop specialized hardware specifically designed for Threshold Neurons to optimize their computational paradigm. This hardware, leveraging Threshold Neurons’ efficient designs, would outperform traditional GPU setups and, with robust software support similar to PyTorch, greatly enhance AI infrastructure compatibility.

FPGA Implementation for Inference. While this paper does not primarily focus on domain-specific circuit design, we contend that the inherent simplicity of Threshold Neurons offers significant advantages for hardware design. To validate this advantage, we employ an FPGA-based proof-of-concept implementation.

In GPU implementations, the CUDA kernel abstracts the functionality of weighted-sum kernels or layers; conversely, FPGA implementations are neuron-grained, operating at the level of individual neurons. Initially, we develop a single-neuron circuit using Verilog HDL. We encapsulate the polarity of each neuron separately into a port for random initialization. Additionally, we encapsulate all thresholds in the neuron as input ports for convenient weights programming.

Due to the unity of Threshold-Net, a single circuit prototype suffices for the entire FPGA implementation. By reusing this circuit prototype, we construct various sizes of weighted-sum kernels or layers, corresponding to the instantiation in

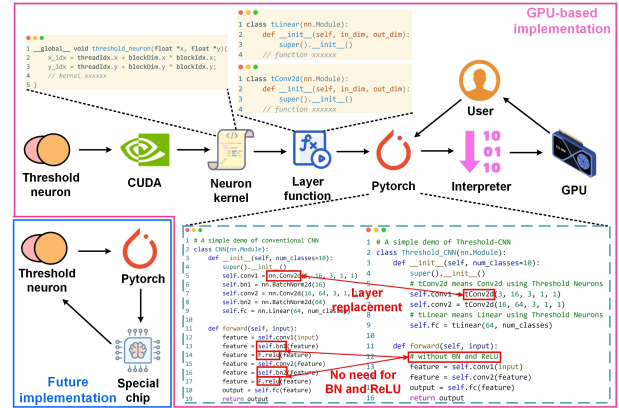


Figure 5: Implementation of Threshold Neurons and Threshold-Net.

hardware design. By integrating these implemented kernels or layers, we achieve the complete implementation of Threshold-Net on FPGA.

The high efficiency of FPGA implementation is manifested in two key aspects: high inference efficiency and high design efficiency. Our experimental results, as detailed in Section 5, demonstrate a high inference efficiency. The use of only one circuit prototype throughout underscores the implementation’s high design efficiency.

5 EVALUATION

In this section, we assess Threshold Neurons through software and hardware experiments across a range of tasks. We aim to determine if the novel neuron design can effectively address diverse modeling tasks like conventional DNNs, and investigate whether our design can enhance efficiency.

5.1 Experimental Setup

5.1.1 Image Dataset. We selected multiple image datasets to evaluate the performance of Threshold-Net. For image classification tasks, we selected four datasets: CIFAR10 [18], MNIST [11], SVHN [26], and Fashion-MNIST [39]. For image generation tasks, we selected the MNIST [11] and Fashion-MNIST [39] datasets as examples.

5.1.2 Sensing Dataset. For near-sensor tasks, we selected six common sensing datasets: UniMiB SHAR [24], UCI-HAR [6], PAMAP2 [29], USC-HAD [45], Daily and Sports Activities (DASA) [2], OPPORTUNITY [31], and WISDM [37]. We first segment these datasets and then pre-process the data, including data cleaning, merging, and re-formatting.

5.1.3 Network Architecture. We use existing network architectures to test Threshold-Net, including simple CNN, ResNet18 [14], and Diffusion model, shown in Table 2. For image classification tasks, we choose ResNet18 and modify

the channel width to make ResNet18 more suitable for simple image classification tasks, reducing the risk of over-fitting. For image generation tasks, we extend Threshold Neurons to the Diffusion model. We use simple CNN for sensing tasks. For FPGA implementation, we construct a 4-layer neural network for deployment and evaluation.

Table 2: Network Architectures Used in Evaluations of Threshold-Net. "CONV3(64)" means kernel size is 3 and channels are 64. FC represents fully-connected layers. "BasicBlock" represents the conventional block in ResNet. "N3(5)" means a layer with 5 neurons, each neuron has 3 input channels and so on.

Network	Architecture
Simple CNN	CONV3(64)-CONV3(128)-CONV3(256)-CONV3(512)-FC-FC
4-layer NN	N3(5)-N5(3)-N3(1)-N1(1)
Resnet18-FW64	CONV3(16)-BasicBlock(32)-BasicBlock(64)-BasicBlock(64)
Resnet18-FW128	CONV3(32)-BasicBlock(64)-BasicBlock(128)-BasicBlock(128)
Resnet18-FW256	CONV3(64)-BasicBlock(128)-BasicBlock(256)-BasicBlock(256)
Diffusion	TimeEmbedding-UNet

5.1.4 Hardware Simulation at Kernel Level. To demonstrate the advantages of Threshold Neurons in hardware, we construct circuits for different sizes of kernels, containing Threshold Neurons. The circuits are based on Verilog, and we use Synopsys DC for synthesis. We conduct power consumption and area simulations using the TSMC 28nm PDK, with a frequency limitation of 50MHz. For comparison, we also construct circuits for different sizes of kernels, containing conventional artificial neurons.

5.1.5 FPGA-based Implementation at System Level. We use FPGA to construct a system using Threshold Neurons. We select Xilinx PYNQ-Z2 as the hardware platform. We use Threshold Neurons to form a 4-layer neural network and deploy its circuit prototype on FPGA. We use Vivado to measure the power consumption and latency of Threshold Neurons after place-and-route.

5.1.6 Baseline and Evaluation Index. For image classification tasks, we select DenseShift [20], ShiftAddNet [42], AdderNet [7], and DeepShift [13] as the baselines because they are all multiplication-less networks. We compare the accuracy, number of multiplications (Mul), and neuron types of Threshold-Net with that of baselines. We also compare Threshold-Net with ResNet18 under structured pruning methods to show the advantage of efficient neuron design.

For image generation tasks, we train a conventional diffusion model as a comparison and use Fréchet Inception Distance (FID) as the evaluation index. For sensing tasks, we train simple CNN and compare its accuracy with that of Threshold-Net.

5.2 Results of Image Classification Tasks

5.2.1 Inference Performance on GPU. We conduct inference performance tests on Nvidia GeForce RTX 4090, with results outlined in Table 3. In comparison to the baselines, Threshold-Net demonstrates SOTA accuracy. The baselines incorporate various neuron types, including normalization or traditional weighted-sum neurons, resulting in non-zero multiplication counts. Conversely, Threshold-Net consists solely of a single neuron type. Owing to the absence of normalization, the number of multiplications in Threshold-Net is reduced to zero. Threshold Neurons and Threshold-Net successfully meet the design objective of efficiency and unity, contrasting with the diverse neuron types present in the baseline models.

5.2.2 Training Performance on GPU. We evaluate the training performance using Nvidia GeForce RTX 4090. While we propose GPU implementation of Threshold-Net, it incurs a relatively high training overhead, as illustrated in Figure 6. The training speed per epoch and the convergence rate are slower than those of conventional DNNs due to inadequate GPU support. Nevertheless, given that mobile and edge devices are typically utilized for inference rather than training, our emphasis should focus on inference efficiency.

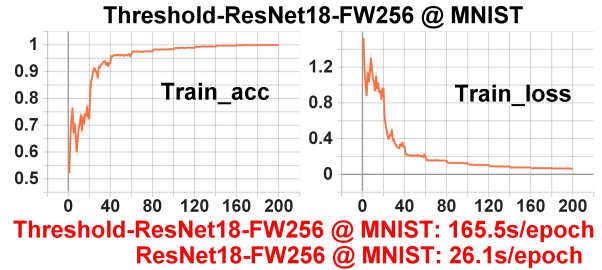


Figure 6: Curves of Threshold-Net during Training.

5.2.3 Quantization. We test the quantization of Threshold Neurons to ensure that Threshold-Net can be deployed on existing hardware. We use an 8-bit uniform and symmetrical quantization method and quantize weights per tensor. The weights of artificial neurons will show as a Gaussian distribution, while the weights of subtraction-based neurons will show as a Laplacian distribution [43]. From Figure 7, the distribution of Threshold-Net weights is near the Laplacian distribution. The results show that Threshold Neurons and Threshold-Net are compatible with quantization methods without accuracy loss.

Table 3: The Results of Image Classification Tasks. "FW" means final width of channel dimensions. Baselines use BNs or traditional weighted-sum neurons in their network architecture, thus containing multiplications. "Neuron type" means how many kinds of neurons are in the network.

	Model	Mul	Neuron type	Dataset	Acc
Baseline	DenseShift-ResNet18-FW256	2919.44K	5	CIFAR10	85.64%
	ShiftAddNet-ResNet18-FW256	118.80K	5		82.45%
	AdderNet-ResNet18-FW256	2531.36K	6		80.03%
	DeepShift-ResNet18-FW256	148.30K	4		64.91%
Ours	Threshold-ResNet18-FW64	0	1	CIFAR10	83.56% ↓ 2.08%
	Threshold-ResNet18-FW128	0	1		86.71% ↑ 1.07%
	Threshold-ResNet18-FW256	0	1		88.53% ↑ 2.89%
Baseline	DenseShift-ResNet18-FW256	2230.64K	5	MNIST	99.15%
	ShiftAddNet-ResNet18-FW256	99.60K	5		99.10%
	AdderNet-ResNet18-FW256	1942.16K	6		99.04%
	DeepShift-ResNet18-FW256	98.84K	4		97.82%
Ours	Threshold-ResNet18-FW64	0	1	MNIST	99.05% ↓ 0.10%
	Threshold-ResNet18-FW128	0	1		99.16% ↑ 0.01%
	Threshold-ResNet18-FW256	0	1		99.19% ↑ 0.04%
Baseline	DenseShift-ResNet18-FW256	2230.64K	5	Fashion-MNIST	91.27%
	ShiftAddNet-ResNet18-FW256	99.60K	5		90.90%
	AdderNet-ResNet18-FW256	1942.16K	6		90.88%
	DeepShift-ResNet18-FW256	98.84K	4		87.73%
Ours	Threshold-ResNet18-FW64	0	1	Fashion-MNIST	91.37% ↑ 0.10%
	Threshold-ResNet18-FW128	0	1		91.96% ↑ 0.69%
	Threshold-ResNet18-FW256	0	1		92.13% ↑ 0.86%
Baseline	DenseShift-ResNet18-FW256	2919.44K	5	SVHN	91.15%
	ShiftAddNet-ResNet18-FW256	118.80K	5		91.67%
	AdderNet-ResNet18-FW256	2531.36K	6		90.52%
	DeepShift-ResNet18-FW256	148.30K	4		68.03%
Ours	Threshold-ResNet18-FW64	0	1	SVHN	91.54% ↑ 0.39%
	Threshold-ResNet18-FW128	0	1		92.04% ↑ 0.89%
	Threshold-ResNet18-FW256	0	1		92.56% ↑ 1.41%

5.2.4 Comparison with Pruning. Table 4 shows the results of the comparison between Threshold-Net and structured pruning. Although the pruned models have high sparsity, they still retain a large amount of multiplications, which is still inefficient for hardware. Threshold-Net has no multiplications and is more efficient.

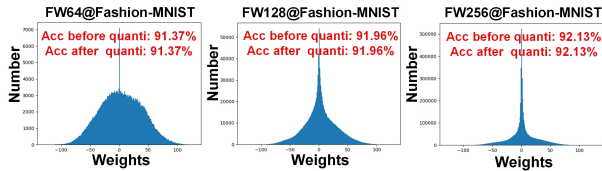


Figure 7: Threshold-Net Weights Distribution after Quantization.

Table 4: The results of comparison with pruning at CIFAR10 dataset. The sparsity comes from structured pruning.

Model	Acc	Sparsity
ResNet18-FW64	91.05%	0%
ResNet18-FW64	83.12%	50.75%
Threshold-ResNet18-FW64	83.56%	–
ResNet18-FW128	92.64%	0%
ResNet18-FW128	86.68%	59.90%
Threshold-ResNet18-FW128	86.71%	–
ResNet18-FW256	93.80%	0%
ResNet18-FW256	88.70%	66.43%
Threshold-ResNet18-FW256	88.53%	–

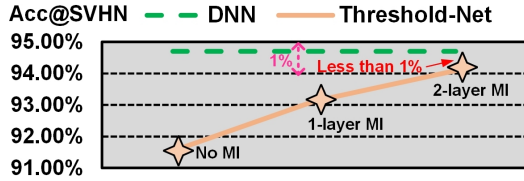


Figure 8: Fitting capability of Threshold-Net with MI. "1-layer MI" means using MI to replace the first CONV3. "2-layer MI" means using MI to replace the first CONV3 and the last FC.

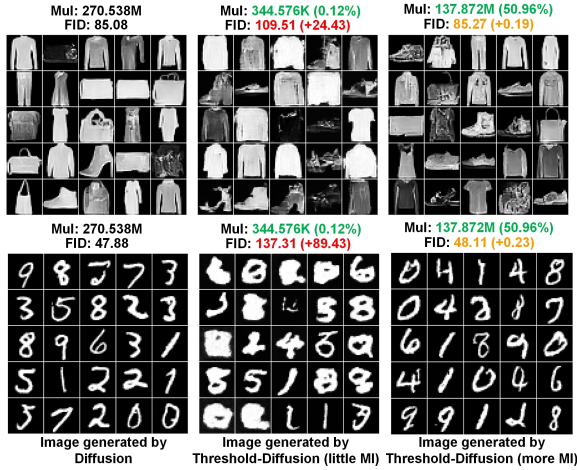


Figure 9: Images generated by Diffusion and Threshold-Diffusion. "Little MI" means using MI to replace all timestep embedding layers. "More MI" means using MI to replace both timestep embedding layers and the first layer of each block.

5.2.5 Fitting Capability with MI. MI mixes the Threshold Neurons and multiplication-based neurons, enhancing the fitting capability of Threshold-Net. We test the improvement of fitting capability with layer-wise MI, as shown in Figure 8. The results demonstrate that by applying MI to just two layers (the first and the last), Threshold-Net can nearly match the fitting capability of multiplication-based networks, with less than a 1% discrepancy.

5.3 Results of Image Generation Tasks

Due to the complexity of the generation tasks, we use MI in Threshold-Diffusion. When we use little MI in Threshold-Net, the FID of generated images increases significantly. However, when we use more MI in Threshold-Net, the FID can be recovered to its original level (Diffusion model using artificial neurons), as shown in Figure 9. That means Threshold-Net with proper MI mechanism can achieve complex tasks. Moreover, Threshold-Net only uses 50.96% multiplications, showing its high efficiency.

Table 5: Results of Sensing Tasks.

Dataset	Network	Acc
UniMiB SHAR	CNN	82.60%
	Threshold-CNN	81.23% ↓ 1.37%
UCI-HAR	CNN	95.21%
	Threshold-CNN	92.70% ↓ 2.51%
PAMAP2	CNN	90.67%
	Threshold-CNN	91.90% ↑ 1.23%
USC-HAD	CNN	86.51%
	Threshold-CNN	88.65% ↑ 2.14%
DASA	CNN	85.80
	Threshold-CNN	87.24% ↑ 1.44%
OPPORTUNITY	CNN	82.88
	Threshold-CNN	84.60% ↑ 1.72%
WISDM	CNN	97.46
	Threshold-CNN	97.51% ↑ 0.05%

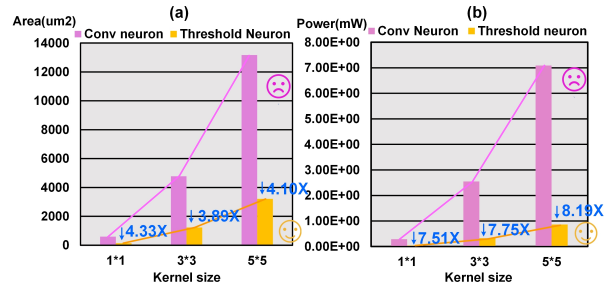


Figure 10: Hardware Simulation Results of Threshold Neurons. "5*5" means a convolution kernel whose kernel size is 5, containing 25 neurons, and so on.

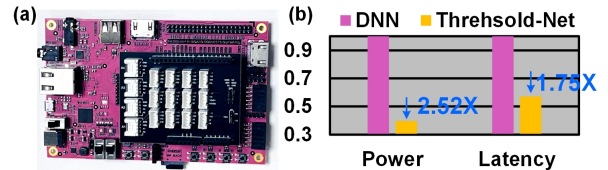


Figure 11: (a) PYNQ-7020 FPGA Platform. (b) Results on FPGA. The frequency of the system is limited to 50 MHz.

5.4 Results of Sensing Tasks

The results of sensing tasks are shown in Table 5. In four sensing datasets, Threshold-CNN shows improved accuracy in some datasets, while in two cases, it experiences accuracy degradation of 1.37% and 2.51%, respectively. In addition, Threshold-CNN is hardware-efficient and effective, which is more suitable for near-sensor computing scenarios on embedded devices.

5.5 Results of Hardware Simulation

5.5.1 Area. The Area results are shown in Figure 10 (a). We choose three kernels of different sizes and achieve their

circuits. From Figure 10 (a), Threshold Neurons save $3.89\times \sim 4.33\times$ hardware area. Area saving allows for more space in hardware design, effectively improving the computing power of a single chip under the same area.

5.5.2 Power. The power results are shown in Figure 10 (b). Threshold Neurons save $7.51\times \sim 8.19\times$ circuit energy at kernel level. These results indicate that Threshold Neurons suit the low-power requirement of mobile/edge circumstances, leveraging less energy to achieve DNN computing.

5.6 Threshold-Net on FPGA

5.6.1 Power. Due to the multiplication-free design and the threshold mechanism in Threshold Neurons, Threshold-Net achieves $2.52\times$ power savings at the system level, as shown in Figure 11 (b). The power saving will become more salient as the number of neurons increases.

5.6.2 Latency. From Figure 11 (b), Threshold-Net achieves $1.75\times$ speedup at the system level. As the layers get deeper, the speedup will increase. The hardware simulation is kernel-level, while the implementation of FPGA is an end-to-end system, thus leading to different results. Overall, Threshold-Net shows its efficient and high-speed performance on FPGA.

6 RELATED WORK

6.1 Hardware-efficient Neural Network

DNN models are based on heavy multiplications for feature extraction and data processing, which are high-cost and inefficient. Current works try to design hardware-efficient networks, focusing on reducing multiplications. Many works [13, 20, 42] use shift-based operations to replace multiplications. However, these shift-based networks require each weight to be a power of two. The weight distribution in these networks is restricted. Unlike these, Threshold Neurons use subtractions to replace multiplications rather than using shift operations. Some works [16, 27] use 1-bit quantization, which can effectively simplify the multiplications. Low-bit quantization often requires retraining or other methods to estimate gradients for optimization. Unlike these, Threshold Neurons fundamentally address the basic reasons for inefficiency and are orthogonal to common quantization methods.

6.2 On-device Inference

With the development of AI, mobile/edge devices with sensors are gaining emerging applications, such as Human Action Recognition (HAR), and industrial fault monitoring. However, existing DNNs require huge hardware resources, posing challenges for executing inference on mobile/edge devices. Existing works [1, 15, 19] utilize model compression techniques to reduce hardware requirements. They then employ memory management or model partitioning methods to enable

inference on mobile/edge devices. Yet, these works overlook the fundamental issue that multiplication-based neurons are the source of inefficiency. We propose a new type of neuron that is efficient and unified, addressing the fundamental problem.

6.3 Brain-inspired Computing

Brain-inspired models strive to replicate the human brain’s computational paradigm to enhance computational efficiency. Spiking Neural Networks (SNNs) exemplify this approach. SNNs encode information both in the timing and rate of spikes. In contrast, Threshold Neurons are designed to handle static input-output mappings at each layer, thereby simplifying implementation while maintaining efficiency. In SNNs, the computation of the spike decision occurs post-aggregation of inputs. Conversely, Threshold Neurons utilize a pre-aggregation threshold mechanism, individually comparing each input to a set threshold. This method can filter out unimportant information in advance, boosting neuron efficiency. SNNs employ a Heaviside step function for activation, which is non-differentiable, thus requiring surrogate gradient methods [25] or non-gradient-based learning techniques for training [4, 38]. In contrast, Threshold Neurons preserve differentiability and facilitate seamless integration with standard DNNs, enabling the use of conventional optimization techniques.

7 DISCUSSION AND FUTURE WORK

First, current network architectures may not be ideally suited for integrating Threshold Neurons. We utilized traditional frameworks (shown in Table 2) to demonstrate the potential of Threshold-Net, but the optimal architecture for Threshold Neurons remains undefined. Future efforts will explore using Neural Architecture Search (NAS) and other strategies to develop more effective network configurations for Threshold Neurons. Second, our reliance on CUDA and GPUs is a compromise since these platforms do not fully align with Threshold Neurons’ operational advantages. Experiments on FPGAs reveal significant hardware efficiencies with Threshold Neurons. Developing ASICs specifically designed for Threshold Neurons could further enhance their performance, opening new pathways in hardware design tailored to their unique properties.

8 CONCLUSION

In this paper, we propose Threshold Neurons, which are hardware-efficient, brain-inspired, and unified. We use Threshold Neurons to construct Threshold-Net within existing network architectures. Experiments have shown that Threshold Neurons and Threshold-Net can significantly improve hardware efficiency while achieving commendable accuracy across diverse tasks.

REFERENCES

- [1] Azzam Alhussain and Mingjie Lin. 2023. FPGA-QHAR: Throughput-Optimized for Quantized Human Action Recognition on The Edge. arXiv:arXiv:2311.03390
- [2] Billur Barshan and Kerem Altun. 2013. Daily and Sports Activities. UCI Machine Learning Repository. DOI: <https://doi.org/10.24432/C5C59F>
- [3] James Betker, Gabriel Goh, Li Jing, † TimBrooks, Jianfeng Wang, Linjie Li, † LongOuyang, † JuntangZhuang, † JoyceLee, † YufeiGuo, † WesamManassra, † PrafullaDhariwal, † CaseyChu, † YunxinJiao, and Aditya Ramesh. [n. d.]. Improving Image Generation with Better Captions. <https://api.semanticscholar.org/CorpusID:264403242>
- [4] Guoqiang Bi and Mu ming Poo. 1998. Synaptic Modifications in Cultured Hippocampal Neurons: Dependence on Spike Timing, Synaptic Strength, and Postsynaptic Cell Type. *The Journal of Neuroscience* 18 (1998), 10464 – 10472. <https://api.semanticscholar.org/CorpusID:16317084>
- [5] William Ted Brown, Leslie B. Gordon, Michael W. Glynn, Michael R. Erdos, Christiane M. Robbins, Tracy Y. Moses, Peter Berglund, Amalia S. Dutra, Evgenia D. Pak, Sandra G. Durkin, Antonei B Csoka, Michael Boehnke, Thomas W. Glover, and Francis S. Collins. [n. d.]. Turning on and off recurrent balanced cortical activity. <https://api.semanticscholar.org/CorpusID:7285513>
- [6] Erhan Bulbul, Aydin Cetin, and Ibrahim Alper Dogru. 2018. Human Activity Recognition Using Smartphones. In *2018 2nd International Symposium on Multidisciplinary Studies and Innovative Technologies (ISMSIT)*. 1–6. <https://doi.org/10.1109/ISMSIT.2018.8567275>
- [7] Hanting Chen, Yunhe Wang, Chunjing Xu, Boxin Shi, Chao Xu, Qi Tian, and Chang Xu. 2019. AdderNet: Do We Really Need Multiplications in Deep Learning? CVPR 2020. (2019). arXiv:arXiv:1912.13200
- [8] Ping Chi, Shuangchen Li, Cong Xu, Tao Zhang, Jishen Zhao, Yongpan Liu, Yu Wang, and Yuan Xie. 2016. PRIME: A Novel Processing-in-Memory Architecture for Neural Network Computation in ReRAM-Based Main Memory. In *2016 ACM/IEEE 43rd Annual International Symposium on Computer Architecture (ISCA)*. 27–39. <https://doi.org/10.1109/ISCA.2016.13>
- [9] Maurizio Ferrarri Dacrema, Paolo Cremonesi, and Dietmar Jannach. 2019. Are We Really Making Much Progress? A Worrying Analysis of Recent Neural Recommendation Approaches. *CoRR* abs/1907.06902 (2019). arXiv:1907.06902 <http://arxiv.org/abs/1907.06902>
- [10] Prasanna Date, Thomas Potok, Catherine Schuman, and Bill Kay. 2022. Neuromorphic Computing is Turing-Complete. In *Proceedings of the International Conference on Neuromorphic Systems 2022 (ICONS '22)*. Association for Computing Machinery, New York, NY, USA, Article 16, 10 pages. <https://doi.org/10.1145/3546790.3546806>
- [11] Li Deng. 2012. The MNIST Database of Handwritten Digit Images for Machine Learning Research [Best of the Web]. *IEEE Signal Processing Magazine* 29, 6 (2012), 141–142. <https://doi.org/10.1109/MSP.2012.2211477>
- [12] Marat Dukhan. 2019. The Indirect Convolution Algorithm. *CoRR* abs/1907.02129 (2019). arXiv:1907.02129 <http://arxiv.org/abs/1907.02129>
- [13] Mostafa Elhoushi, Zihao Chen, Farhan Shafiq, Ye Henry Tian, and Joey Yiwei Li. 2021. DeepShift: Towards Multiplication-Less Neural Networks. In *IEEE Conference on Computer Vision and Pattern Recognition Workshops, CVPR Workshops 2021, virtual, June 19-25, 2021*. Computer Vision Foundation / IEEE, 2359–2368. <https://doi.org/10.1109/CVPRW53098.2021.00268>
- [14] Kaiming He, Xiangyu Zhang, Shaoqing Ren, and Jian Sun. 2016. Deep Residual Learning for Image Recognition. In *2016 IEEE Conference on Computer Vision and Pattern Recognition (CVPR)*. 770–778.
- [15] Kai Huang and Wei Gao. 2022. Real-time neural network inference on extremely weak devices: agile offloading with explainable AI. In *Proceedings of the 28th Annual International Conference on Mobile Computing And Networking (MobiCom '22)*. Association for Computing Machinery, New York, NY, USA, 200–213. <https://doi.org/10.1145/3495243.3560551>
- [16] Itay Hubara, Daniel Soudry, and Ran El Yaniv. 2016. Binarized Neural Networks. arXiv:arXiv:1602.02505
- [17] Seonjun Kim, Minjae Kim, and Youngki Lee. 2023. A Joint Analysis of Input Resolution and Quantization Precision in Deep Learning. In *Proceedings of the 29th Annual International Conference on Mobile Computing and Networking, ACM MobiCom 2023, Madrid, Spain, October 2-6, 2023*, Xavier Costa-Pérez, Joerg Widmer, Diego Perino, Domenico Giustiniano, Haitham Al-Hassanieh, Arash Asadi, and Landon P. Cox (Eds.). ACM, 146:1–146:3. <https://doi.org/10.1145/3570361.3615753>
- [18] Alex Krizhevsky. 2009. Learning Multiple Layers of Features from Tiny Images. <https://api.semanticscholar.org/CorpusID:18268744>
- [19] Xiangyu Li, Yuanchun Li, Yuanzhe Li, Ting Cao, and Yunxin Liu. 2024. FlexNN: Efficient and Adaptive DNN Inference on Memory-Constrained Edge Devices. In *Proceedings of the 30th Annual International Conference on Mobile Computing and Networking (ACM MobiCom '24)*. Association for Computing Machinery, New York, NY, USA, 709–723. <https://doi.org/10.1145/3636534.3649391>
- [20] Xinlin Li, Bang Liu, Rui Heng Yang, Vanessa Courville, Chao Xing, and Vahid Partovi Nia. 2023. DenseShift : Towards Accurate and Efficient Low-Bit Power-of-Two Quantization. In *IEEE/CVF International Conference on Computer Vision, ICCV 2023, Paris, France, October 1-6, 2023*. IEEE, 16964–16974. <https://doi.org/10.1109/ICCV51070.2023.01560>
- [21] Zhou C Liang J, Yang Z. 2024. Excitation–Inhibition Balance, Neural Criticality, and Activities in Neuronal Circuits. *The Neuroscientist*. DOI: doi:10.1177/10738584231221766.
- [22] Shuying Liu and Weihong Deng. 2015. Very deep convolutional neural network based image classification using small training sample size. In *2015 3rd IAPR Asian Conference on Pattern Recognition (ACPR)*. 730–734. <https://doi.org/10.1109/ACPR.2015.7486599>
- [23] W. Liu, Dragomir Anguelov, D. Erhan, Christian Szegedy, Scott E. Reed, Cheng-Yang Fu, and Alexander C. Berg. 2015. SSD: Single Shot MultiBox Detector. In *European Conference on Computer Vision*. <https://api.semanticscholar.org/CorpusID:2141740>
- [24] Daniela Micucci, Marco Mobilio, and Paolo Napoletano. 2016. UniMiB SHAR: a new dataset for human activity recognition using acceleration data from smartphones. arXiv:arXiv:1611.07688
- [25] Emre O. Neftci, Hesham Mostafa, and Friedemann Zenke. 2019. Surrogate Gradient Learning in Spiking Neural Networks: Bringing the Power of Gradient-Based Optimization to Spiking Neural Networks. *IEEE Signal Processing Magazine* 36, 6 (2019), 51–63. <https://doi.org/10.1109/MSP.2019.2931595>
- [26] Yuval Netzer, Tao Wang, Adam Coates, A. Bissacco, Bo Wu, and A. Ng. 2011. Reading Digits in Natural Images with Unsupervised Feature Learning. <https://api.semanticscholar.org/CorpusID:16852518>
- [27] Mohammad Rastegari, Vicente Ordonez, Joseph Redmon, and Ali Farhadi. 2016. XNOR-Net: ImageNet Classification Using Binary Convolutional Neural Networks. arXiv:arXiv:1603.05279
- [28] Joseph Redmon, Santosh Kumar Divvala, Ross B. Girshick, and Ali Farhadi. 2015. You Only Look Once: Unified, Real-Time Object Detection. *2016 IEEE Conference on Computer Vision and Pattern Recognition (CVPR)* (2015), 779–788. <https://api.semanticscholar.org/CorpusID:206594738>
- [29] Attila Reiss. 2012. PAMAP2 Physical Activity Monitoring. UCI Machine Learning Repository. DOI: <https://doi.org/10.24432/C5N2W2H>.
- [30] Joohong Rhee, Dayoung Choi, and Hyunggon Park. 2024. Poster: Symmetrical Pruning for Lightweight Network Anomaly Detector.

- In *Proceedings of the 22nd Annual International Conference on Mobile Systems, Applications and Services, MOBISYS 2024, Minato-ku, Tokyo, Japan, June 3-7, 2024*, Tadashi Okoshi, JeongGil Ko, and Robert LiKamWa (Eds.). ACM, 634–635. <https://doi.org/10.1145/3643832.3661395>
- [31] Daniel Roggen, Nguyen-Dinh Calatroni, Alberto, Ricardo Long-Van, Chavarriaga, and Hesam Sagha. 2012. OPPORTUNITY Activity Recognition. UCI Machine Learning Repository. DOI: <https://doi.org/10.24432/C5M027>.
- [32] Caio S. Rohwedder, João P. L. de Carvalho, José Nelson Amaral, Guido Araújo, Giancarlo Colmenares, and Kai-Ting Amy Wang. 2021. Pooling Acceleration in the DaVinci Architecture Using Im2col and Col2im Instructions. In *IEEE International Parallel and Distributed Processing Symposium Workshops, IPDPS Workshops 2021, Portland, OR, USA, June 17-21, 2021*. IEEE, 46–55. <https://doi.org/10.1109/IPDPSW52791.2021.00016>
- [33] Chitwan Saharia, William Chan, Saurabh Saxena, Lala Li, Jay Whang, Emily Denton, Seyed Kamyar Seyed Ghasemipour, Burcu Karagol Ayan, S. Sara Mahdavi, Raphael Gontijo Lopes, Tim Salimans, Jonathan Ho, David J. Fleet, and Mohammad Norouzi. 2022. Photorealistic Text-to-Image Diffusion Models with Deep Language Understanding. *CoRR* abs/2205.11487 (2022). <https://doi.org/10.48550/ARXIV.2205.11487> arXiv:2205.11487
- [34] Ali Shafiee, Anirban Nag, Naveen Muralimanohar, Rajeev Balasubramanian, John Paul Strachan, Miao Hu, R. Stanley Williams, and Vivek Srikumar. 2016. ISAAC: A Convolutional Neural Network Accelerator with In-Situ Analog Arithmetic in Crossbars. In *2016 ACM/IEEE 43rd Annual International Symposium on Computer Architecture (ISCA)*. 14–26. <https://doi.org/10.1109/ISCA.2016.12>
- [35] Manli Sun, Zhanjie Song, Xiaoheng Jiang, Jing Pan, and Yanwei Pang. 2017. Learning Pooling for Convolutional Neural Network. *Neurocomput.* 224, C (feb 2017), 96–104. <https://doi.org/10.1016/j.neucom.2016.10.049>
- [36] Christian Szegedy, Wei Liu, Yangqing Jia, Pierre Sermanet, Scott Reed, Dragomir Anguelov, Dumitru Erhan, Vincent Vanhoucke, and Andrew Rabinovich. 2015. Going deeper with convolutions. In *2015 IEEE Conference on Computer Vision and Pattern Recognition (CVPR)*. 1–9. <https://doi.org/10.1109/CVPR.2015.7298594>
- [37] Gary Weiss. 2019. WISDM Smartphone and Smartwatch Activity and Biometrics Dataset. UCI Machine Learning Repository. DOI: <https://doi.org/10.24432/C5HK59>.
- [38] Yujie Wu, Lei Deng, Guoqi Li, Jun Zhu, and Luping Shi. 2017. Spatio-Temporal Backpropagation for Training High-Performance Spiking Neural Networks. *Frontiers in Neuroscience* 12 (2017). <https://api.semanticscholar.org/CorpusID:6446489>
- [39] Han Xiao, Kashif Rasul, and Roland Vollgraf. 2017. Fashion-MNIST: a Novel Image Dataset for Benchmarking Machine Learning Algorithms. arXiv:arXiv:1708.07747
- [40] Lingxi Xie, Qi Tian, John Flynn, Jingdong Wang, and Alan Yuille. 2016. Geometric Neural Phrase Pooling: Modeling the Spatial Co-occurrence of Neurons. In *Computer Vision – ECCV 2016*, Bastian Leibe, Jiri Matas, Nicu Sebe, and Max Welling (Eds.). Springer International Publishing, Cham, 645–661.
- [41] Mingshan Xue, Bassam V. Atallah, and Massimo Scanziani. 2014. Equalizing Excitation-Inhibition Ratios across Visual Cortical Neurons. *Nature* 511 (2014), 596 – 600. <https://api.semanticscholar.org/CorpusID:4458376>
- [42] Haoran You, Xiaohan Chen, Yongan Zhang, Chaojian Li, Sicheng Li, Zihao Liu, Zhangyang Wang, and Yingyan Lin. 2020. ShiftAddNet: A Hardware-Inspired Deep Network. *ArXiv* abs/2010.12785 (2020). <https://api.semanticscholar.org/CorpusID:225067910>
- [43] Haoran You, Baopu Li, Huihong Shi, Yonggan Fu, and Yingyan Lin. 2022. ShiftAddNAS: Hardware-Inspired Search for More Accurate and Efficient Neural Networks. In *International Conference on Machine Learning, ICML 2022, 17-23 July 2022, Baltimore, Maryland, USA (Proceedings of Machine Learning Research)*, Kamalika Chaudhuri, Stefanie Jegelka, Le Song, Csaba Szepesvári, Gang Niu, and Sivan Sabato (Eds.), Vol. 162. PMLR, 25566–25580. <https://proceedings.mlr.press/v162/you22a.html>
- [44] Lei Zhang, Shuai Wang, and B. Liu. 2018. Deep learning for sentiment analysis: A survey. *Wiley Interdisciplinary Reviews: Data Mining and Knowledge Discovery* 8 (2018). <https://api.semanticscholar.org/CorpusID:10694510>
- [45] Mi Zhang and Alexander A. Sawchuk. 2012. USC-HAD: a daily activity dataset for ubiquitous activity recognition using wearable sensors. *Proceedings of the 2012 ACM Conference on Ubiquitous Computing* (2012). <https://api.semanticscholar.org/CorpusID:6870922>
- [46] Pengfei Zhang, Dingzhu Wen, Guangxu Zhu, Qimei Chen, Kaifeng Han, and Yuanming Shi. 2024. Collaborative Edge AI Inference over Cloud-RAN. *CoRR* abs/2404.06007 (2024). <https://doi.org/10.48550/ARXIV.2404.06007> arXiv:2404.06007
- [47] Shuai Zhang, Lina Yao, Aixin Sun, and Yi Tay. 2019. Deep Learning Based Recommender System: A Survey and New Perspectives. *ACM Comput. Surv.* 52, 1, Article 5 (feb 2019), 38 pages. <https://doi.org/10.1145/3285029>
- [48] Xiaomao Zhou, Qingmin Jia, and Renchao Xie. 2022. NestFL: efficient federated learning through progressive model pruning in heterogeneous edge computing. In *ACM MobiCom '22: The 28th Annual International Conference on Mobile Computing and Networking, Sydney, NSW, Australia, October 17 - 21, 2022*. ACM, 817–819. <https://doi.org/10.1145/3495243.3558248>
- [49] Rui-Jie Zhu, Yu Zhang, Ethan Sifferman, Tyler Sheaves, Yiqiao Wang, Dustin Richmond, Peng Zhou, and Jason K. Eshraghian. 2024. Scalable MatMul-free Language Modeling. arXiv:arXiv:2406.02528